Stability of symmetric and asymmetric vortex pairs over slender conical wings and bodies

Jinsheng Cai,[a] Shijun Luo, and Feng Liu[b]
Department of Mechanical and Aerospace Engineering, University of California, Irvine, California 92697-3975

(Received 30 December 2002; accepted 21 October 2003; published online 7 January 2004)

Theoretical analyses are presented for the stability of symmetric and asymmetric vortex pairs over slender conical wings and bodies under small perturbations in an inviscid incompressible flow at high angles of attack and sideslip. The three-dimensional problem of a pair of vortices over slender conical wings and bodies is reduced to a problem in two dimensions by using the conical flow assumption and classical slender-body theory. The stability of symmetric and asymmetric vortex pairs over flat-plate delta wings, slender circular cones, and elliptic cones of various thickness ratios are examined. Results are compared with available experimental data. © *2004 American Institute of Physics.* [DOI: 10.1063/1.1637601]

I. INTRODUCTION

Separation vortices over highly swept slender wings and bodies at high angles of attack are known to greatly increase the lift coefficient. However, the initially symmetric vortex pair may become asymmetric as the angle of attack is increased beyond a certain value, causing large rolling moments in the case of swept wings or large side forces in the case of slender bodies even at zero roll and yawing angles. The transition of the vortex pattern from being symmetric to asymmetric is of major importance for the performance and control of aircraft and other flight vehicles capable of extreme maneuvers. Much experimental, theoretical, and computational work has been spent on the understanding, prediction, and control of the onset of vortex asymmetry. The basic physical mechanism of this transition, however, is not clear. At least two possible causes for the vortex asymmetry were suggested mainly based on experimental investigations: (1) Inviscid hydrodynamic instability of the symmetrically separated vortices (Keener and Chapman)[1] and (2) asymmetric flow separation and/or asymmetric flow reattachment on each side of the body (Ericsson).[2] There is at present no general agreement on the mechanism involved in the creation of the flow asymmetry.

Using a vortex line or a vortex sheet model, Dyer *et al.*[3] Fiddes,[4] and Fiddes and Williams[5] found stationary asymmetric as well as symmetric vortex pairs over slender conical bodies even though the separation lines were assumed to be symmetrical. Although their findings support the existence of conical asymmetric vortices, these vortices may be subject to instabilities that may prevent their stable appearance in reality.

Pidd and Smith[6] studied a spatial type of stability of the symmetric and asymmetric vortices found in Dyer *et al.*,[3] in which they introduced small disturbances of the positions and strengths of the vortices and determined their stability by looking at the growth of such disturbances along the vortices in the downstream direction.

The present authors[7] developed a general stability condition for vortices in a two-dimensional incompressible inviscid flow field. A mathematical framework was presented to reduce the problem of a three-dimensional potential flow over slender conical bodies at high angles of attack to the solution of a two-dimensional problem. The two-dimensional stability condition was then extended to analyzing the absolute (temporal) stability of symmetric vortex pairs over three-dimensional slender conical bodies. The bodies considered included circular cones and highly swept flat-plate wings with and without vertical fins, and elliptic cones of various eccentricities. Results based on the theory agreed well with known experimental observations. The analyses showed that adding a fin of sufficient height had a stabilizing effect on the symmetric vortices over a circular cone or a flat-plate delta wing. However, a fin of nonzero but low height would destabilize the vortices. These findings agreed with the known experimental observations by Stahl,[8] Ng,[9] and Asghar *et al.*[10] of the stabilizing effect of fins of sufficient heights in their experiments. At the same time, the findings also clarified the conflict between the experimental observations by Shanks[11] and Stahl *et al.*[12] Shanks[11] reported asymmetric vortices in his flat-plate delta wing, whereas Stahl *et al.*[12] observed none until vortex breakdown in their tests. It was found that Shanks' model[11] differed from that by Stahl *et al.*[12] in that Shanks' model had a short center spline which, according to the analysis in Ref. 7, would destabilize the symmetric vortices. Analyses of elliptic cones in Ref. 7 also showed the stabilizing effect of flattening the nose of a conical body as was found in the experimental works by Edwards[13] and Stahl,[14] and the high sensitivity of the vortex stability to the location of (symmetric) separation near the round leading edges of a thin wing, which most likely were the cause of the loss of symmetry of the vortices over the

[a]Present address: Temasek Laboratories, National University of Singapore, Singapore.
[b]Author to whom correspondence should be addressed; electronic mail: fliu@uci.edu

round-edged flat-plate delta wing of Bird.[15] These studies indicated that an inviscid hydrodynamic instability was responsible for the loss of symmetry of the leading-edge vortices.

Degani and Tobak,[16] Dagani,[17,18] and Levy *et al.*[19] studied the vortices over a slender ogive-cylinder body of revolution by wind-tunnel tests and numerical computations using a time-accurate Navier–Stokes method. They found that it was necessary to maintain a fixed small geometrical disturbance near the body apex in order to obtain and keep an asymmetric vortex pattern in their numerical computations. Once the small artificially introduced geometric ''imperfection'' at the nose tip was removed, the vortices would return to symmetry. This finding in numerical computation, coupled with their experimental observation that the vortex pattern depended continuously on the size and location of the controlled disturbance, led them to believe that the intrinsic geometric imperfections in the nose region of the body and a ''convective'' instability mechanism similar in concept to that studied by Pidd and Smith[6] was responsible for the onset of asymmetry of the otherwise would-be symmetric vortices over a slender body of revolution with a pointed nose.

In a separate numerical study, Hartwich *et al.*[20] reported asymmetric flow field solutions of the incompressible three-dimensional turbulent Navier–Stokes equations for a 3.5 caliber tangent-ogive cylinder at an angle of attack of 40° without the imposition of a fixed ''geometric asymmetry'' in the computations. They claim that the a symmetric solution is triggered by machine round-off error in the computations. Thus, asymmetries can be induced by a small transient disturbance. This route to asymmetry is referred to as an absolute instability. There are experimental observations supporting the notion of absolute instability, for example, the existence of a bistable leeside flow field variation with a roll angle of an ogive cylinder at incidence angles in the range of 50°–60° (Ref. 21) and the hysteresis effects detected in experiments where asymmetric vortex flow patterns over slender bodies of revolution are mirror imaged by suction or blowing.[22,23]

No stability analysis was developed in the above experimental and numerical studies. In the scenario of a convective instability, the originally undisturbed stationary symmetric and asymmetric vortices are conical. However, the spatially disturbed vortices are no longer conical. Pidd and Smith[6] were able to perform analysis of this type of instability by using the slender-body theory. No upstream effect of the disturbance is possible in such an approach. The type of instability studied in Ref. 7 and in the present article refers to a temporal evolution of the conical symmetric or asymmetric vortices. The flow stays conical before or after the disturbance. The disturbances are of a global nature. Satisfaction of this absolute type of stability, as well as the convective type of stability, should be regarded as necessary conditions for any configuration of a conical symmetric or asymmetric vortex pattern to persist in a flow.

It must be pointed out that vortices may also lose symmetry or stability due to vortex breakdown. This happens at very large angles of attack or farther downstream of the body. The mechanisms of vortex breakdown is still not clear and its onset is difficult to predict. However, experimental data support that concentrated vortices over slender conical wings/bodies very often exhibit either the absolute type or the convective-type instabilities before their concentrated vortex structure breaks down far downstream of the wing or at higher angles of attack. The present article is restricted to the study of the absolute type of vortex instability before vortex breakdown sets in.

In this article, we extend our previous stability analysis in Ref. 7 to include asymmetric vortices over slender conical bodies. The general stability conditions for vortices in two dimensions is briefly reviewed. Then, the derivation of the vortex velocity for slender conical wings and bodies is presented along with the method of finding the families of stationary symmetric and asymmetric vortices. The stability of stationary symmetric and asymmetric vortex flows over slender flat-plate delta wings with and without sideslip, and those over circular and elliptic cones with zero sideslip are analyzed in detail by the present theory and compared with available experimental observations.

II. STABILITY CONDITION FOR VORTICES IN TWO DIMENSIONS

The stability condition for vortices in two dimensions developed in Ref. 7 is summarized in this section. Consider a system of vortices in a two-dimensional flow. Assume one of the vortices in the system is located at (x,y). As this vortex is moved in the physical plane, other vortices in the system are assumed to move according to a given mode of motion, for instance, symmetric or antisymmetric mode of motion, subject to given boundary conditions. The starting point for the general stability condition is that given the flow boundary conditions and the mode of vortex motion, one has already obtained the *vortex velocity* (u,v), at which the vortex would move as a function of its location (x,y), i.e., $u=u(x,y)$ and $v=v(x,y)$.

The stationary points (x_0,y_0) for the vortex can be found by solving the equations $u(x_0,y_0)=0$ and $v(x_0,y_0)=0$. When the vortex is perturbed from its stationary point (x_0,y_0) and then let go, the vortex will follow the flow and may either move back to its initial equilibrium position (stable), diverge from its initial equilibrium point (unstable), or move periodically around the equilibrium point or stay at the disturbed position (neutrally stable). If an originally symmetric vortex pair is unstable under small disturbances, we then expect the vortex pair to become asymmetric, nonconical (curvy), or unsteady since they cannot stay at their initial symmetric equilibrium positions in a stable fashion. If the vortex pair is also unstable at initially asymmetric equilibrium positions, the vortices must then be curvy or unsteady.

Define the Jacobian and divergence of the vortex velocity field $\mathbf{q}=(u,v)$,

$$J=\begin{bmatrix} \dfrac{\partial u}{\partial x} & \dfrac{\partial u}{\partial y} \\ \dfrac{\partial v}{\partial x} & \dfrac{\partial v}{\partial y} \end{bmatrix}, \quad D=\nabla\cdot\mathbf{q}=\frac{\partial u}{\partial x}+\frac{\partial v}{\partial y}. \tag{1}$$

TABLE I. Stability condition for vortex motion.

	D_0	J_0	Comment
Stable	<0	>0	
Unstable	>0	any	
	any	<0	
Neutral	$=0$	>0	oscillating
	<0	$=0$	nonoscillating
	$=0$	$=0$	nonoscillating

It can be easily shown that the eigenvalues of this problem are

$$\lambda_{1,2}=\frac{1}{2}(D_0\pm\sqrt{D_0^2-4J_0}), \tag{2}$$

where the subscript 0 denotes values at (x_0,y_0). The stability condition for the vortex motion may then be summarized in Table I. It is useful to note that for a flow to be unstable either $D_0>0$ or $J_0<0$.

Once the *vortex velocity* field $u(x,y)$ and $v(x,y)$ are given, it is straightforward to calculate, either analytically or numerically, the divergence D and the Jacobian J and thus the eigenvalues, λ_1 and λ_2 at any given stationary points. The physical interpretations of D_0 and J_0 in the stability condition of Table I are discussed in Ref. 7, where D_0 and J_0 are directly used to determine stability of various test cases. For convenience, the maximum real part of the two eigenvalues λ_1 and λ_2 in Eq. (2) will be plotted and used to determine stability in this article. A positive value of this variable means instability of the vortex system.

In the consideration of stability for a pair of symmetric or asymmetric vortices, it is sufficient to consider only symmetric and antisymmetric modes of perturbations. This can be shown as below. Let ΔZ_1 and ΔZ_2 be arbitrary displacements of vortex 1 and vortex 2, respectively, on the complex domain. One can always construct a symmetric perturbation: $\Delta S=(\Delta Z_1+\overline{\Delta Z_2})/2$, and an antisymmetric perturbation: $\Delta A=(\Delta Z_1-\overline{\Delta Z_2})/2$, so that both ΔZ_1 and ΔZ_2 can be represented as a linear combination of ΔS and ΔA, i.e., $(\Delta Z_1,\Delta Z_2)=(\Delta S,\overline{\Delta S})+(\Delta A,-\overline{\Delta A})$, where the overbar denotes complex conjugate.

III. THE VORTEX VELOCITY FOR SLENDER CONICAL WINGS AND BODIES

Consider the flow past a slender conical body of an arbitrary symmetric cross section at an angle of attack α and sideslip angle β as shown in Fig. 1. The body may have a slender triangular flat-plate wing passing through the axis of the body. The flow separates from the wing sharp leading edge or body surface along separation lines, and the flow is assumed to be steady, inviscid, incompressible, and conical.

We consider a pair of two concentrated vortices on the leeside of the body. The distributed vortex sheets that connect the separation lines and the two concentrated vortices are neglected since their strength is in general much smaller than that of the two concentrated vortices. On the other hand, the two concentrated vortices can be approximated as a pair

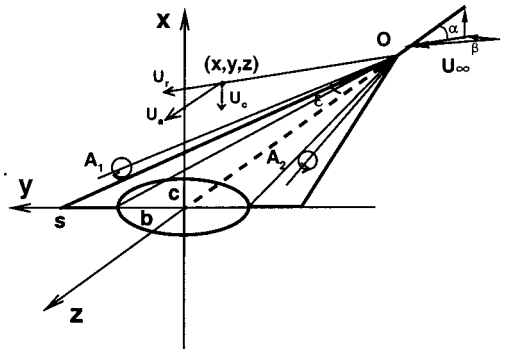

FIG. 1. Slender conical wing-body combination and separation vortices.

of vortex lines OA_1 and OA_2, which are also assumed to be rays from the body apex O under the conical flow assumption. Secondary separation vortices are also neglected.

The inviscid incompressible flow considered in the above model is irrotational except at the centers (cores) of the isolated vortices. The governing equation for the velocity potential is the three-dimensional Laplace equation with zero normal flow velocity on the body surface and the Kutta condition at sharp edges as the boundary conditions. By the principle of superposition, the flow around the body can be obtained by solving the following two flow problems: (1) The flow due to the normal component of the freestream velocity, and (2) the flow due to the axial component of the freestream velocity, both subject to the above boundary conditions. We denote the velocity field of the first problem by $\mathbf{U}_1$ and that of the second problem by $\mathbf{U}_2$.

In the first problem, the slender body is placed normal to the cross flow components $U_x=U_\infty\cos\beta\sin\alpha$ and $U_y=U_\infty\sin\beta$. Since the body is assumed to be slender, the velocity in the z direction due to three-dimensional effects can be neglected. The flow in each cross section at z may then be regarded as a two-dimensional flow across the local cross sectional profile governed by the two-dimensional Laplace equation with the appropriate boundary conditions. Solution to this two-dimensional velocity field can be obtained by conformal mapping or other analytical or numerical methods. For the simple profiles, such as an ellipse, $\mathbf{U}_1$ can be easily obtained by conformal mapping. The conformal mapping for this profile in the plane Z to a circle of unit radius in a uniform flow of velocity $(U_x/2,U_y/2)$ in the plane ζ is

$$Z=\frac{1}{2}\left(\zeta+\frac{\lambda}{\zeta}\right),$$

where $c=1+\lambda/2$ and $b=1-\lambda/2$ are the semi-axes of the ellipse along the x and y axes. The complex velocity expression of $\mathbf{U}_1$ is

$$u-iv=\left[\frac{1}{2}\left(\overline{U_n}-\frac{U_n}{\zeta^2}\right)+\frac{i\Gamma_1}{2\pi}\left(\frac{1}{\zeta-\zeta_1}-\frac{1}{\zeta-1/\overline{\zeta_1}}\right)-\frac{i\Gamma_2}{2\pi}\left(\frac{1}{\zeta-\zeta_2}-\frac{1}{\zeta-1/\overline{\zeta_2}}\right)\right]\left(\frac{d\zeta}{dZ}\right),$$

where $U_n=U_x(1+iK_S)$; $K_S=\tan\beta/\sin\alpha$ is the sideslip similarity parameter; ζ_1 and ζ_2, and Γ_1 and Γ_2 are the positions and strengths of the vortex 1 and vortex 2, respectively.

As shown in Fig. 1, the second problem corresponds to the flow past a conical body with an axial freestream velocity $U_a=U_\infty\cos\beta\cos\alpha$. According to the analysis of the authors,[7] the velocity $\mathbf{U}_2$ can be written in the nonorthogonal conical coordinate system (x',y',r') as

$$\mathbf{U}_2(x,y,z)=\mathbf{U}_p(x',y')+\mathbf{U}_c(x',y')+u_{r'}(x',y')\mathbf{e}_{r'}, \quad (3)$$

where $x'=x/s$ and $y'=y/s$, s is the semispan of the wing or body in the $x-y$ plane at z, and $\mathbf{e}_{r'}$ is the unit vector in the ray direction. The complex velocity expression of $\mathbf{U}_c(x',y')$ is,

$$u_c-iv_c=-\frac{U_x\overline{Z}}{sK}, \quad (4)$$

where K is the Sychev similarity parameter (Sychev)[24]

$$K=\tan\alpha/\tan\varepsilon. \quad (5)$$

The velocity $\mathbf{U}_c$ represents the flow velocity drawn toward the body axis when the axial flow is decomposed into a velocity along the conical ray and the velocity in the cross-sectional plane. At the surface of the body, the normal component of this velocity must be canceled by the potential field $\mathbf{U}_p$. Physically, $\mathbf{U}_p$ represents the displacement effect of a nonzero thickness body. $\mathbf{U}_p$ can be obtained by a singularity method in the two-dimensional plane (x,y) subject to the boundary condition $\mathbf{U}_p\cdot\mathbf{n}_c=-\mathbf{U}_c\cdot\mathbf{n}_c$, where $\mathbf{n}_c$ is the normal vector to the two-dimensional cross sectional profile of the body at a given z. The complex velocity at the point $Z=x+iy$ due to N point sources within the body contour at $Z_j=x_j+iy_j$ can be written as

$$u_p-iv_p=\frac{1}{2\pi}\sum_{j=1}^{N}\frac{Q_j}{Z-Z_j}, \quad (6)$$

where Q_j is the strength of the point sources and $Q_j(j=1,2,...N)$ are to be determined by N simultaneous equations of the boundary condition on the body contour.

Notice that $\mathbf{U}_1$ and $\mathbf{U}_2$ depend only on x' and y', and the $u_{r'}\mathbf{e}_{r'}$ term in Eq. (3) is a velocity component in the ray direction $\mathbf{e}_{r'}$ which does not contribute to the flow velocity in the plane $(\mathbf{e}_{x'},\mathbf{e}_{y'})$. Consequently, the stability of the flow system can be analyzed by studying only the two-dimensional "flow field" in the plane (x',y'). The complex velocity at the vortex point Z_1 (or ζ_1) and Z_2 (or ζ_2) are obtained by a limiting process (see Rossow).[25]

$$u_1-iv_1=\left[\frac{1}{2}\left(\overline{U_n}-\frac{U_n}{\zeta_1^2}\right)+\frac{i\Gamma_1}{2\pi}\left(-\frac{1}{\zeta_1-1/\overline{\zeta_1}}\right)-\frac{i\Gamma_2}{2\pi}\left(\frac{1}{\zeta_1-\zeta_2}-\frac{1}{\zeta_1-1/\overline{\zeta_2}}\right)\right]\left(\frac{d\zeta}{dZ}\right)_1-\frac{i\Gamma_1}{4\pi}\left(\frac{d^2Z}{d\zeta^2}\right)_1\left(\frac{d\zeta}{dZ}\right)_1^2-\frac{U_x\overline{Z_1}}{sK}+\frac{1}{2\pi}\sum_{j=1}^{N}\frac{Q_j}{Z_1-Z_j}, \quad (7)$$

where the subscript 1 denotes the values at $Z=Z_1$ (or $\zeta=\zeta_1$), and

$$u_2-iv_2=\left[\frac{1}{2}\left(\overline{U_n}-\frac{U_n}{\zeta_2^2}\right)-\frac{i\Gamma_2}{2\pi}\left(\frac{1}{-\zeta_2-1/\overline{\zeta_2}}\right)+\frac{i\Gamma_1}{2\pi}\left(\frac{1}{\zeta_2-\zeta_1}-\frac{1}{\zeta_2-1/\overline{\zeta_1}}\right)\right]\left(\frac{d\zeta}{dZ}\right)_2+\frac{i\Gamma_2}{4\pi}\left(\frac{d^2Z}{d\zeta^2}\right)_2\left(\frac{d\zeta}{dZ}\right)_2^2-\frac{U_x\overline{Z_2}}{sK}+\frac{1}{2\pi}\sum_{j=1}^{N}\frac{Q_j}{Z_2-Z_j}, \quad (8)$$

where the subscript 2 denotes the values at $Z=Z_2$ (or $\zeta=\zeta_2$).

The stationary positions, Z_1 (or ζ_1) and Z_2 (or ζ_2), and strengths of the vortices, Γ_1 and Γ_2, are determined by solving a set of algebraic equations. These are $u_1-iv_1=0$ and $u_2-iv_2=0$ for the vortex velocity fields, and two more equations that set the flow velocities to zero at postulated separation points on a smooth body or finite values at the sharp edges of a thin wing (Kutta condition). The four algebraic equations are linear in Γ_1 and Γ_2, and nonlinear in Z_1 (or ζ_1) and Z_2 (or ζ_2). They are solved by an iteration method. A Newton iteration for the vortex locations is constructed for $\mathbf{F}(\mathbf{X})=0$, where $\mathbf{F}=[u_1,v_1,u_2,v_2]^T$, $\mathbf{X}=[\xi_1,\eta_1,\xi_2,\eta_2]^T$, $\zeta_1=\xi_1+i\eta_1$, and $\zeta_2=\xi_2+i\eta_2$. Given the vortex positions ζ_1 and ζ_2, the vortex strengths Γ_1 and Γ_2 can be obtained by using the separation conditions.

Once the stationary positions, Z_{10} and Z_{20}, of the two vortices are determined, the vortex stability condition listed in Table I may then be readily applied to the vortex velocities (u_1,v_1) and (u_2,v_2) of the vortices Z_1 and Z_2, respectively, under small perturbations around their stationary positions. The perturbations are decomposed into a symmetric perturbation

$$Z_1=Z_{10}+\Delta Z, \quad Z_2=Z_{20}+\overline{\Delta Z}, \quad (9)$$

and an antisymmetric perturbation

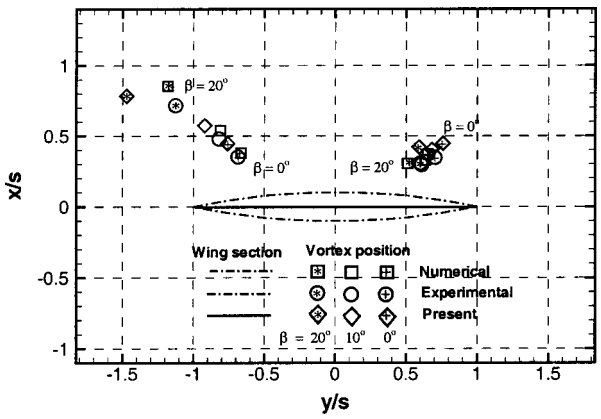

FIG. 2. Location of stationary asymmetric vortex pairs over a delta wing with sideslip angles $\beta=0°$, 10°, and 20° for $K=1.5$.

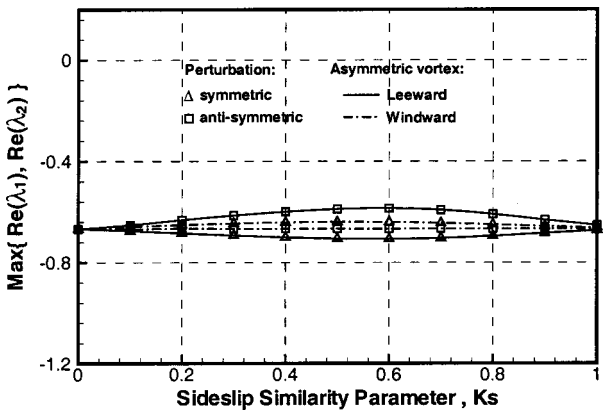

FIG. 3. Maximum real part of eigenvalues of asymmetric vortex pairs over a delta flat-plate wing vs K_S for $K=1.5$.

$$Z_1=Z_{10}+\Delta Z, \quad Z_2=Z_{20}-\overline{\Delta Z}, \tag{10}$$

where $\Delta Z=\Delta x+i\Delta y$, $|\Delta x|\ll s$, and $|\Delta y|\ll s$.

IV. ANALYSIS OF TYPICAL MODEL CONFIGURATIONS

This section discusses the application of the above theory to a number of model configurations typical of aeronautical applications.

A. Flat-plate delta wing at nonzero sideslip

Huang and Chow[26] and the present authors[7] showed the existence of symmetric vortex pairs over highly swept flat-plate delta wings at high angles of attack and proved that they were stable under small perturbations. Asymmetric solutions are sought and examined in this article.

No stationary asymmetric vortex solutions are found without sideslip based on the present model. The originally symmetric vortex pair under zero sideslip, however, becomes asymmetric under nonzero sideslip. In addition, no other branches of asymmetric vortex solutions are found.

Verhaagen and Naarding[27] studied by low-speed wind-tunnel experiment and a slender-body free-vortex sheet method a sharp-edged thin delta wing of 76° sweep at a constant angle of attack of $\alpha=21.1°$ and angles of sideslip β ranging from 0° to 20°, i.e., sideslip similarity parameter K_S ranging from 0 to 1. The geometry of the forward half of the wing is nearly conical. Perpendicular to the root chord the cross sections of the wing model were circular biconvex. The maximum thickness of the wing was 3.2% of the root chord. The wing is approximated by a flat plate in the present analysis. Verhaagen and Naarding[27] measured and computed by their slender-body free-vortex sheet method the locations of the vortices over this wing at the cross section $x=0.6$ of the root chord. The given angle of attack corresponds to $K=1.5$. Figure 2 compares the locations of the vortex pairs obtained by the present method based on a flat-plate wing with the numerical and experimental results by Verhaagen and Naarding.[27] The experimental Reynolds number is 2.5×10^6 based on the root chord. The trend of the movements of the windward and leeward vortices against the angle of sideslip are well predicted by the present analysis. As the sideslip similarity parameter K_S grows, the windward vortex moves inboard and remains nearly the same distance above the upper surface of the wing and the leeward vortex moves outboard and upward from the wing. Verhaagen and Naarding[27] observed in their experiment (Fig. 4 of Ref. 27) that the windward leading edge vortex breaks down and touches the trailing edge of the wing when β reaches 12°. The differences in magnitude of the movement between the values predicted by the present analysis and the experimental data are mainly due to this vortex breakdown, which the present theory cannot account for. The neglect of the vortex sheets connecting the leading edge and the concentrated vortex and the wing thickness distribution in the present analysis also may have contributed to the differences.

Figure 3 shows the maximum real part of the two eigenvalues of the asymmetric vortex pair over a flat-plate delta wing with $K=1.5$. The asymmetric vortex pair are stable for the whole range of K_S from 0 to 1, which agrees with the experimental observations by Verhaagen and Naarding.[27] They showed that the leading edge vortices of the wing are stationary and stable before vortex breakdown (Figs. 1 and 4 in Ref. 27). The degree of stability of both vortices is almost independent of K_S at the given constant K.

Figure 4 shows the variation of eigenvalues versus K for a given $K_S=0.5$. The asymmetric vortex pair is stable over

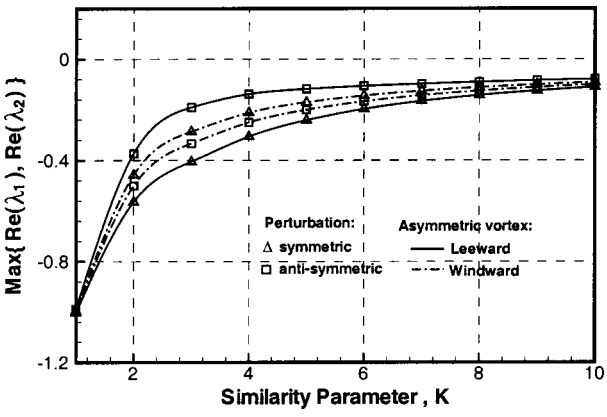

FIG. 4. Maximum real part of eigenvalues of asymmetric vortex pairs over a flat-plate delta wing vs K for $K_S=0.5$.

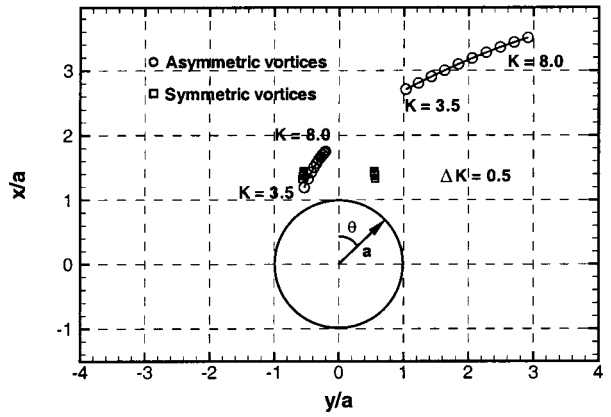

FIG. 5. Location of stationary symmetric and asymmetric vortex pairs over a circular cone for $K=3.5-8.0$ with a 0.5 interval; $\theta_0=45°$ and $K_S=0$.

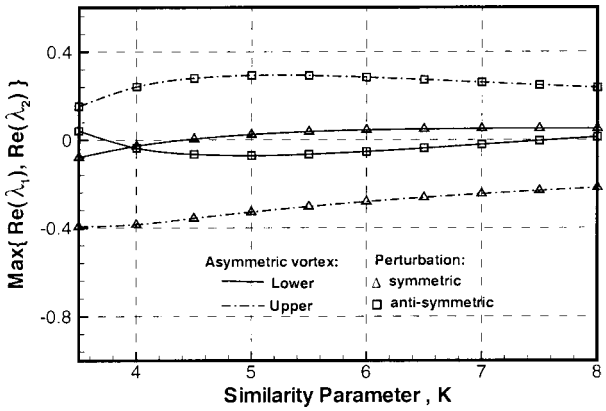

FIG. 6. Maximum real part of eigenvalues of asymmetric vortex pairs over a circular cone vs K for $\theta_0=45°$ and $K_S=0.0$.

the entire range of $1\leqslant K<10$. However, the degree of stability for both vortices decreases as K is increased.

Asymmetric families of solutions are searched within a wide range of the parameter space (K,K_S). As pointed out earlier, no stationary asymmetric vortex solutions are found without sideslip for flat-plate delta wings based on the present model and the only family of stationary asymmetric vortices under nonzero sideslip are those that are originally symmetric under zero sideslip and they are always stable (before vortex breakdown) based on the present stability analysis.

B. Circular cones

Symmetric vortex pairs about circular and elliptic cones were studied in Ref. 7. We extend the analyses to asymmetric vortex pairs.

Unlike in the case of the flat-plate delta wing, asymmetric stationary vortices are found at zero sideslip and with symmetric separations for both circular and not very flat elliptic cones under large angles of attack. Figure 5 plots the locations of stationary symmetric and asymmetric vortex pairs over a circular cone with symmetric separations at $\theta_0=45°$ (θ_0 is measured from the leeward side of the incidence plane), for $K=3.5-8$ and $K_S=0$ (zero sideslip). The square and circle symbols denote symmetric and asymmetric vortex locations, respectively. No stationary asymmetric vortex solutions are found when $K\leqslant 3$, while there exist stationary symmetric vortex solutions once K is greater than 1, as were found in Ref. 7. The two separation vortices have different heights and strengths. The upper vortex moves outboard and the lower vortex moves inboard when K is increased. This is consistent with the direction of induced velocity by each other of the two vortices.

For each stationary asymmetric vortex pair shown in Fig. 5, there is another stationary solution in which the positions of the starboard and port board vortices are swapped due to symmetry of the body with respect to the vertical center plane (the incidence plane). In addition to the family of asymmetric solutions shown in Fig. 5 (including their mirror images), a second family of stationary asymmetric solutions is found. However, the distance from the body axis to the farther-away vortex in such a solution is one order of magnitude greater than the body radius at the same axial location. Such stationary vortex solutions contradict the assumption of slender-body flow of the current model. Therefore, they are discarded here. This note applies in similar places below.

It was shown in Ref. 7 that stationary symmetric vortex pairs over a circular cone at zero sideslip ($K_S=0$) are stable under symmetric perturbations and unstable under antisymmetric perturbations for any $K>1$. Figure 6 plots the eigenvalues versus K for asymmetric vortex pairs with $\theta_0=45°$ and $K_S=0.0$. The upper vortex is stable under symmetric perturbations, but unstable under antisymmetric perturbations. The lower vortex is stable only when $K\leqslant 4.4$ under symmetric perturbations. Under antisymmetric perturbations, it is stable for $3.7\leqslant K\leqslant 7.5$. Thus the vortex pair are not stable since there is at least one vortex that is not stable under either a symmetric or antisymmetric perturbation. An extensive parameter search has been performed of various symmetric and asymmetric separation positions and K values. However, no stable solutions are obtained. This suggests that there exist no stable conical asymmetric vortex pairs for the circular cone at high angles of attack with either symmetric or asymmetric separation positions within the assumption of the present vortex model and the definition of the present linear time-wise instability.

Jenista and Nelson[28] measured the vortex positions over a cone with rear fins using smoke and laser-produced light sheet for $\alpha=25°$, 35°, 45°, and 55°. The vortices were symmetric straight lines for $\alpha=25°$ and 35°. Although the present authors[7] showed the effect of full-length conical fins in suppressing instability of symmetric vortices over circular cones and delta wings, it is not clear how important the partial rear mounted fins were for maintaining the symmetric conical vortices in this case. However, Jenista and Nelson[28] found that vortices became asymmetric and nonconical when $\alpha=45°$ and 55°. At $\alpha=45°$, the lower vortex was curved in the top view, while the upper vortex remained straight. At $\alpha=55°$, both the lower and upper vortices became curved. Ericsson and Reding[29] also noted experimental data that showed oscillatory variation of the total side force of a slender circular cone with angle of attack, even to the degree of

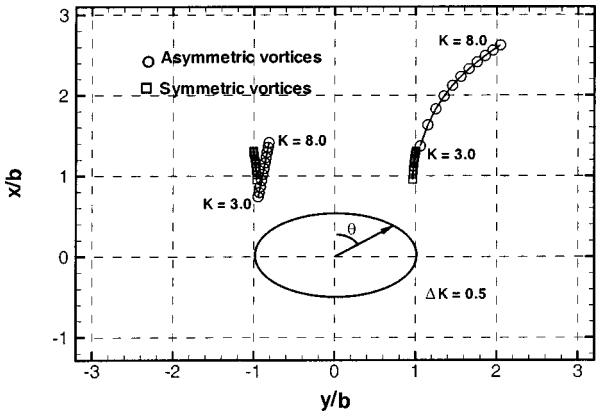

FIG. 7. Location of stationary symmetric and asymmetric vortex pairs over an elliptic cone with $K=3.0-8.0$ with a 0.5 interval; $\tau=c/b=0.5$, $\theta_0=85°$, and $K_S=0$.

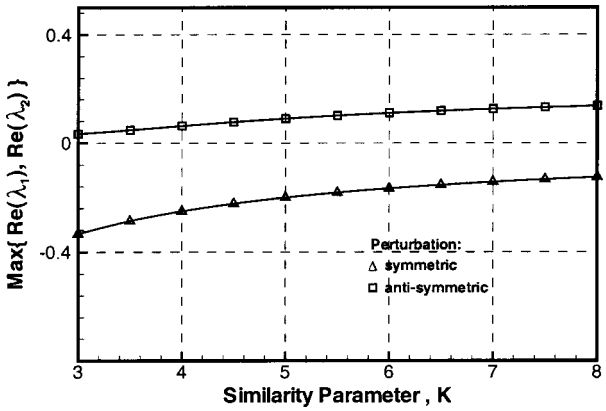

FIG. 8. Maximum real part of eigenvalues of symmetric vortex pairs over an elliptic cone vs K; $\tau=c/b=0.5$, $\theta_0=85°$, and $K_S=0$.

changing sign. They commented that this was ''the likely result of a multicell local side force distribution'' along the longitudinal axis of the body, indicating nonconical vortex patterns. Those observations agree with the present findings that there are no stable asymmetric conical vortices over the circular cone. If there are stable vortices, they cannot stay conical.

The above theoretical predictions, however, does not agree fully with experimental results reported by Lowson and Ponton[30] and Pidd and Smith,[6] where they noted observations of both conical and nonconical symmetric and asymmetric vortices over a circular cone. Using the line-vortex model of Dyer *et al.*[3] for slender bodies, Pidd and Smith[6] also studied the stability to small spatial disturbances of conical symmetric and asymmetric vortices over a circular cone with symmetric separation lines on the body. They found that, for most conditions, symmetric vortices were unstable while asymmetric vortices were stable to small spatial disturbances. However, the present temporal stability analyses suggest that all stationary symmetric and asymmetric conical vortex solutions are subject to the global type of instability defined in this article and Ref. 7. Although the two types of stabilities, or rather instabilities, discussed in Pidd and Smith[6] and the present paper, are different in nature, each of them should be regarded as a necessary condition for the existence of stable conical solutions. The discrepancies of the present theoretical analyses, as well as those by Pidd and Smith,[6] from the limited experimental observations for strict circular cones remain to be clarified.

C. Elliptic cones

Studies in Ref. 7 have shown that the degree of instability of the symmetric vortices over a slender elliptic cone decreases monotonically as the cross section is flattened from a thickness ratio of 1 (circle) to 0 (flat plate). For a given K and a separation angle, there is a critical thickness ratio below which the symmetric vortices become stable. These predictions agree well with experimental findings of Stahl[14] and Lowson and Ponton.[30]

We extend our previous studies to asymmetric vortices over elliptic cones under zero sideslip ($K_S=0$). Consider an elliptic cone of semi-apex angle ε measured in the top view at an angle of attack α. Figure 7 shows the elliptic cross section of the body with a thickness ratio $\tau=c/b=0.5$ and the locations of the stationary symmetric and asymmetric vortex pairs found by the present method for K ranging from 3 to 8 with postulated symmetric separation lines at $\theta_0=85°$. In this case, no stationary asymmetric vortex solutions are found for $K\leqslant 2.5$, while stationary symmetric vortex solutions do exist when $K\leqslant 2.5$ as was the case in the studies of Ref. 7.

Figure 8 shows the eigenvalues of the vortex system versus K for the symmetric vortex pairs shown in Fig. 7. The symmetric vortices over the elliptic cone are stable under small symmetric perturbations and unstable under small antisymmetric perturbations. Figure 9 shows the eigenvalues for the asymmetric vortex pairs of the same case. The two vortices are unstable for $K>4.9$. The upper vortex remains unstable while the lower vortex becomes stable when K is reduced below 4.9. Therefore, it is concluded that both the symmetric and asymmetric vortex solutions are unstable under small perturbations for the similarity parameter K up to 8 for this elliptic cone with symmetric separation positions.

As the thickness ratio is reduced, we may expect some of the asymmetric as well as symmetric vortices become

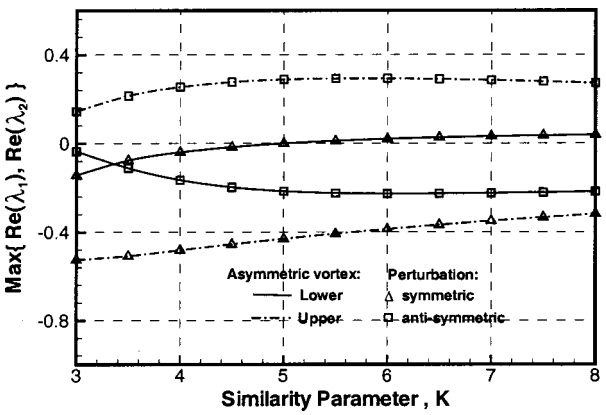

FIG. 9. Maximum real part of eigenvalues of asymmetric vortex pairs over an elliptic cone vs K; $\tau=c/b=0.5$, $\theta_0=85°$, and $K_S=0$.

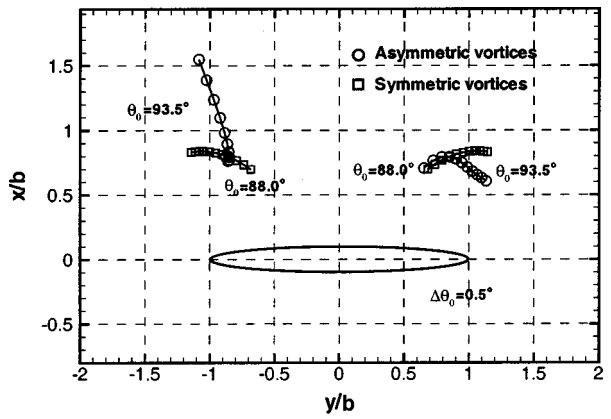

FIG. 10. Location of stationary symmetric and asymmetric separation vortex pairs over an elliptic cone; symmetric vortices are with symmetric separation angles $\theta_0=88.0°-93.5°$ with a 0.5 interval; asymmetric vortices are with left $\theta_0=90.0°$ and right $\theta_0=88.0°-93.5°$ with a 0.5 interval; $\tau=c/b=0.1$, $K=4$, and $K_S=0$.

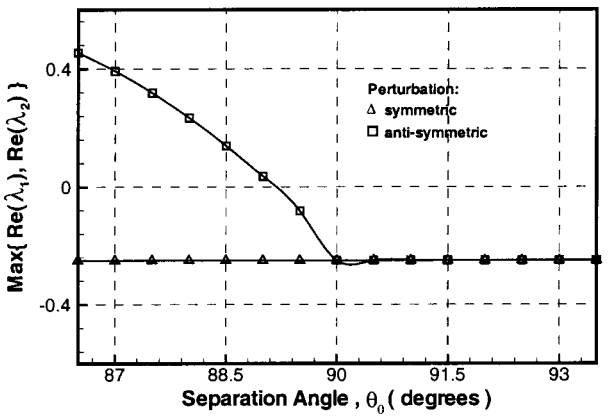

FIG. 11. Maximum real part of eigenvalues of symmetric separation vortex pairs over an elliptic cone vs the (symmetric) separation angle θ_0; $\tau=c/b=0.1$, $K=4$, and $K_S=0$.

stable. Consider the elliptic cone with a thickness ratio of $\tau=0.1$. Figure 10 shows the locations of the stationary symmetric and asymmetric vortex pairs for different separation angles at $K=4$. For such a thin elliptic cone, the flow tends to approach that of the flat-plate delta wing case. No stationary asymmetric vortex solutions are found at zero sideslip when the separation lines are assumed to be symmetric. Only symmetric solutions are found. The symmetric vortices shown in Fig. 10 are obtained with symmetric separation angles ranging from 88.0° to 93.5°. The stationary asymmetric vortex solutions are found only with asymmetric separation lines. The left-hand side separation line is fixed at $\theta_0=90°$ and the right-hand side separation angle is varied from 88.0° to 93.5°. In the symmetric separation case, when θ_0 is increased from 90°, i.e., the separation points move from the leading edge of the wing toward the windward side, the symmetric vortex pair moves outboard and upward, and when θ_0 is decreased from 90°, i.e., the separation points move from the leading edge of the wing toward the leeward side, the symmetric vortex pair moves inboard and downward. In the asymmetric separation case, where the left-hand side θ_0 is fixed at 90°, when the right-hand side θ_0 is increased from 90°, the right vortex moves outboard but downward and the left vortex moves outboard and upward, and when the right θ_0 is decreased from 90°, the right vortex moves inboard and downward and the left vortex moves slightly outboard.

Lee *et al.*[31] controlled the leading edge vortex pair of a delta wing by manipulating the boundary layer flow over the wing leading edges using micromachined actuators in low-speed wind-tunnel tests. The test Reynolds number ranged from 2.1×10^5 to 8.4×10^5 based on the wing root chord. The flow visualization experiments displayed in Figs. 19 and 20 of Ref. 31 showed that when the actuator was activated at a windward location on one side of the wing, the separation position moves windward and the core of the vortex moved significantly outboard and upward on that side relative to the uncontrolled vortex. When the actuator is activated at a leeward location, the separation position moves leeward and the core of the vortex shifted inboard and downward relative to the uncontrolled vortex. Activation of the actuators promoted flow separation. The trends of the predicted vortex movement shown in Fig. 10 of the present analysis agree with the experimental observations. Advantage was taken of such movements of the asymmetric vortex pair generated by slight shifts of the separation positions to generate appreciable aerodynamic moments along all three axes for flight control by Lee *et al.*[31]

Figure 11 plots the eigenvalues of the vortex system versus the separation angle θ_0 for the symmetric vortex pairs. The vortices are stable when the separation is exactly at the leading edge of the cone, i.e., $\theta_0=90°$. The vortices remain stable when the separation points move to the windward side of the cone. However, the vortices become unstable if the separation points wonder slightly over to the leeward side of the cone at $\theta_0<89.17°$. The location of this critical separation point is almost at the leading edge of the cone for this small thickness ratio.

Using tuft-grid surveys at low speeds, Bird[15] observed appearance of asymmetric vortex flow over a slender flat-plate delta wing model with a rounded leading edge and a semi-apex angle $\varepsilon=3.5°$ when $\alpha\geqslant15°$, which disagrees with the observations by Stahl *et al.*,[12] who used wing models with sharp leading edges. Bird[15] did not provide details of his wing profile or measurement of separation angles. As was discussed in Ref. 7, if his wing model were to be represented by our elliptic cone with $\tau=0.1$, the critical separation angle would be $\theta_0=89.3°$ with $K=4.0$ and $\varepsilon=3.5°$ given by his experiment. The asymmetry observed by Bird[15] may be due to such slight changes in the separation position on the round leading edge of his experimental models. This agrees with the experimental results of Lim *et al.*[32] on flat-plate wing of ogive-shaped planform with sharp/rounded tip and edges, which showed that the leading-edge geometry played a crucial role in developing the vortex asymmetry rather than the apex geometry as suggested by Stahl *et al.*[12]

Figure 12 plots the eigenvalues of the asymmetric vortex system versus the right separation angle θ_0. The right vortex is stable when θ_0 is between 89.2° and 92.7° and unstable otherwise. The left vortex is stable when θ_0 is between 88.5° and 91.5° and unstable otherwise. Therefore, the asymmetric

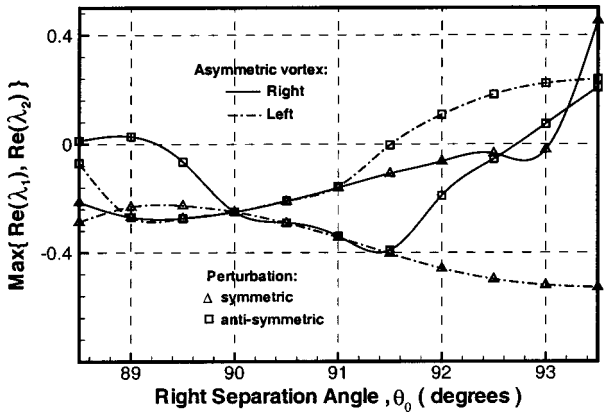

FIG. 12. Maximum real part of eigenvalues of asymmetric separation vortex pairs over an elliptic cone vs the right separation angle θ_0; $\tau=c/b=0.1$, left $\theta_0=90°$, $K=4$, and $K_S=0$.

vortex pair is stable when the right separation angle θ_0 is between 89.2° and 91.5°.

V. CONCLUSIONS

The stability theory developed by the present authors in Ref. 7 for vortex pairs over conical slender bodies in an inviscid, incompressible, and steady flow at high angles of attack is applied to study the stability of symmetric and asymmetric vortex pairs over flat-plate delta wings, slender circular cones, and elliptic cones of various thickness ratios. The following conclusions are drawn.

(1) Stationary symmetric vortex pairs over a flat-plate delta wing at zero sideslip are always stable. No stationary asymmetric vortex pairs exist for a flat-plate delta wing without sideslip. With nonzero sideslip, the originally symmetric vortex pairs become asymmetric but remain stable under any small perturbations.

(2) Both symmetric and asymmetric conical vortex pairs exist over slender circular cones at large angles of attack with either symmetric or asymmetric separations but none of them are stable. An implication is that a stable asymmetric vortex pair over a circular cone at sufficiently high angles of attack shall be in general nonconical or curved. This may explain the large number of experiments where asymmetric curved vortices appear over circular cones and ogive cylinders. However, it also conflicts with the observation of some symmetric and asymmetric conical vortex pairs in a few limited experiments of circular cones. Further investigation is needed to clarify this discrepancy.

(3) Flattening the cross section of a circular cone in the transverse direction improves the stability of the vortices. There exists an elliptic cone with an intermediate finite thickness ratio between the circular cone and the flat-plate delta wing across which the symmetric vortex pair changes from being unstable to stable for a fixed K and fixed symmetric separation lines. For any fixed K, there is also a critical thickness ratio below which no asymmetric stationary vortex pair can be found under the condition of symmetric separations.

(4) The locations and the stability of the stationary vortex pair over a highly swept thin delta wing with round leading edges are sensitive to slight shifts of the separation positions around the leading edge. When the separation positions on the leading edges are slightly asymmetric the originally symmetric stationary vortex pair becomes largely asymmetric, which can be stable within a certain range of separation angles. This sensitivity can be used for control purposes.

The present theory is limited to the absolute type of stability of conical flows for slender bodies. The theoretical results agree well qualitatively in most cases with available experimental observations. There is, however, presently a lack of detailed quantitative measurements of the vortex flow under well-controlled conditions. It is understood that the theory needs further validation by carefully designed experiments or numerical computations.

[1] E. Keener and G. Chapman, AIAA J. **15**, 1370 (1977).
[2] L. Ericsson, J. Aircr. **29**, 1086 (1992).
[3] D. E. Dyer, S. P. Fiddes, and J. H. B. Smith, Aeronaut. Q. **31**, 293 (1982).
[4] S. Fiddes, *Symposium on the Prediction and Exploitation of Separated Flow* (NASA/LRC, Hampton, VA, 1985), pp. 285–310.
[5] S. Fiddes and A. Williams, *Symposium on the Prediction and Exploitation of Separated Flow* (Royal Aeronautical Society, London, 1989), pp. 31.1–31.17.
[6] M. Pidd and J. H. B. Smith, Vortex Flow Aerodynamics, *AGARD CP-494* (Controller HMSO, London, 1991), pp. 18-1-11.
[7] J. Cai, F. Liu, and S. Luo, J. Fluid Mech. **480**, 65 (2003).
[8] W. Stahl, AIAA J. **28**, 1138 (1990).
[9] T. Ng, J. Aircr. **27**, 844 (1990).
[10] A. Asghar, W. Stahl, and M. Mahmood, AIAA J. **32**, 2117 (1994).
[11] R. Shanks, NASA TN D-1822 (NASA/LRC, Hampton, VA, 1963).
[12] W. Stahl, M. Mahmood, and A. Asghar, AIAA J. **30**, 1027 (1992).
[13] O. Edwards, NASA CR 158936 (NASA/LRC, Hampton, VA, 1978).
[14] W. Stahl, AIAA J. **31**, 966 (1993).
[15] J. Bird, NASA TN D-5045 (NASA/LRC, Hampton, VA, 1969).
[16] D. Degani and M. Tobak, Phys. Fluids A **4**, 2825 (1992).
[17] D. Degani, AIAA J. **29**, 560 (1991).
[18] D. Degani, AIAA J. **30**, 94 (1992).
[19] Y. Levy, L. Hesselink, and D. Degani, AIAA J. **34**, 772 (1996).
[20] P. M. Hartwich, R. M. Hall, and M. J. Hemsch, J. Spacecr. Rockets **28**, 258 (1991).
[21] G. G. Zilliac, D. Degani, and M. Tobak, AIAA J. **29**, 667 (1991).
[22] T. T. Ng and G. N. Malcolm, *Proceedings of the AIAA*, Paper 91-0619 (American Institute of Aeronautics and Astronautics, Washington, D.C., 1991).
[23] J. E. Bernhardt and D. R. Williams, Phys. Fluids A **5**, 291 (1993).
[24] V. Sychev, J. Math. Mech. **24**, 296 (1960).
[25] V. J. Rossow, J. Aircr. **15**, 618 (1978).
[26] M. K. Huang and C. Y. Chow, AIAA J. **34**, 1182 (1996).
[27] N. Verhaagen and S. Naarding, J. Aircr. **26**, 971 (1989).
[28] J. M. Jenista and R. C. Nelson, Air Force Armament Lab. AFATL TR 83-04 (Elgin AFB, FL, 1983).
[29] L. Ericsson and J. Reding, *Tactical Missile Aerodynamics: General Topics*, *Progress in Astronautics and Aeronautics*, edited by M. Hemsh (American Institute of Aeronautics and Astronautics, New York, 1992), Vol. 141, pp. 391–452.
[30] M. Lowson and A. Ponton, AIAA J. **30**, 1576 (1992).
[31] G. B. Lee, C. Shih, Y. C. Tai, C. Liu, A. Huang, and C. M. Ho, J. Aircr. **37**, 697 (2000).
[32] T. Lim, K. Lua, and S. Luo, AIAA J. **39**, 539 (2001).